

Non-Fermi-liquid behavior near a $T = 0$ spin-glass transition

Anirvan M. Sengupta*

AT&T Bell Laboratories, 600 Mountain Avenue, Murray Hill, New Jersey 07974

Antoine Georges†

CNRS-Laboratoire de Physique Théorique de l'Ecole Normale Supérieure, † 24, rue Lhomond, 75231 Paris Cedex 05, France
(Received 2 May 1995)

We study the competition between the Kondo effect and Ruderman-Kittel-Kasuya-Yosida interactions near the zero-temperature quantum critical point of an Ising-like metallic spin glass. We consider the mean-field behavior of various physical quantities. In the “quantum-critical regime” nonanalytic corrections to the Fermi-liquid behavior are found for the specific heat and uniform static susceptibility, while the resistivity and NMR relaxation rate have a non-Fermi-liquid dependence on temperature.

I. INTRODUCTION

The interplay between Kondo screening of localized spins by conduction electrons, and ordering of these spins due to the Ruderman-Kittel-Kasuya-Yosida (RKKY) interaction is a central issue in heavy fermion physics. Recently, a class of systems has been studied^{1,2} in which the ordering temperature is driven to zero as a function of concentration, and the paramagnetic metal displays non-Fermi-liquid (NFL) behavior near this $T = 0$ quantum-critical point. The compound $Y_{1-x}U_xPd_3$ is one of the best documented among these systems.^{1,3} In this case, the low-temperature ordered state is reported to be a spin glass for $x > x_c \simeq 0.2$, while the system remains a paramagnet down to the lowest temperature studied for $x < x_c$. It is still debated^{4,5} whether the NFL behavior of the $Y_{0.8}U_{0.2}Pd_3$ system is a single-ion effect or results from the above competition and the proximity of the $T = 0$ critical point. The aim of this paper is not to resolve this debate for this particular system, but to demonstrate that NFL behavior is indeed a generic feature of the vicinity of a $T = 0$ paramagnetic metal to metallic spin-glass transition. This will be shown by solving specific models at mean-field level.

II. MODELS

The models that we shall study are mean-field versions of the Kondo lattice, with an additional quenched randomness on the exchange interactions between localized spins. We consider localized spins \vec{S}_i on a fully connected lattice of N sites $i = 1, \dots, N$. These spins interact with a bath of conduction electrons. In the model that we shall consider first, a major simplification will be made: the conduction electron bath will be assumed to consist of *independent* “reservoirs” of electrons, with no communication between the reservoirs at different sites. The effect

of releasing this simplifying assumption will be discussed in Sec. IV at the end of this paper. The conduction electrons will be denoted by $c_{k\alpha}^{(i)}$, where $\alpha = \uparrow, \downarrow$ is a spin index, k labels the conduction band orbitals, and the site index (i) labels the reservoir associated with site i . The Hamiltonian of the model reads

$$H_1 = \sum_{k,\alpha,i} \epsilon_k c_{k\alpha}^{(i)+} c_{k\alpha}^{(i)} + J_K \sum_i \vec{S}_i \cdot \vec{s}(i) - \sum_{i<j} J_{ij} S_i^z \cdot S_j^z. \quad (1)$$

In this expression, $\vec{s}(i) \equiv \sum_{\alpha\beta} \sum_{k,k'} \frac{1}{2} c_{k\alpha}^{(i)+} \vec{\sigma}_{\alpha\beta} c_{k'\beta}^{(i)}$ is the conduction electron spin density at site i , and J_K the strength of the Kondo coupling between the localized spins and the conduction electrons (taken to be antiferromagnetic). Besides this coupling, the spins have a direct interaction between one another: the J_{ij} 's are quenched independent random variables with a distribution $P(J_{ij}) \sim \exp(-J_{ij}^2/4NJ^2)$. A further simplification of our model is that only the Ising part of the exchange interaction has been included. For $J_K = 0$, the model reduces to the Sherrington-Kirkpatrick model of a classical Ising spin glass⁶ with a freezing transition at $T_c = J$. In contrast, for $J = 0$, we have a system of independent localized spins, each one being quenched by the Kondo effect with its conduction electron reservoir, and the system has no long-range order down to $T = 0$. We are interested in the intermediate behavior where the spin-glass freezing due to the random exchange competes with the local Kondo effect.

Because the model is fully connected, it can be reduced to a single-site problem after taking the (quenched) average over the realizations of the random couplings. In order to describe also the spin-glass phase, we may introduce replicated variables labeled by indices $a, b = 1, \dots, n$. Using standard techniques,⁷⁻⁹ the single-site effective action is found to be (with obvious notations)

$$\begin{aligned}
S_{\text{eff}} = & - \int_0^\beta d\tau \int_0^\beta d\tau' \sum_{\alpha,a} c_{\alpha,a}^+(\tau) \mathcal{G}_0^{-1}(\tau - \tau') c_{\alpha,a}(\tau') \\
& + J_K \int_0^\beta d\tau \sum_a \vec{S}_a(\tau) \cdot \vec{s}_a(\tau) \\
& - J^2 \int_0^\beta d\tau \int_0^\beta d\tau' \sum_{a,b} S_a^z(\tau) D_{ab}(\tau - \tau') S_b^z(\tau').
\end{aligned} \tag{2}$$

In this equation, \mathcal{G}_0 is simply the bare on-site propagator for the conduction electrons: $\mathcal{G}_0 \equiv \sum_k 1/(i\omega_n - \epsilon_k)$, which can be taken to have the characteristic form associated with a flat band without loss of generality: $\mathcal{G}_0(i\omega_n)^{-1} = i\Gamma \text{sgn}(\omega_n)$. The nonlocal spin interaction D_{ab} must satisfy the following self-consistency condition in the thermodynamic limit $N \rightarrow \infty$:

$$D_{ab}(\tau - \tau') = \langle T S_a^z(\tau) S_b^z(\tau') \rangle_{S_{\text{eff}}}. \tag{3}$$

In the following, we shall mainly be concerned with the paramagnetic phase in which replica symmetry holds, so that $D_{ab}(\tau)$ is nonzero only for $a = b$. In the spin-glass phase, D_{ab} is nonzero (but τ independent) for $a \neq b$, and the Edwards-Anderson order parameter is given by $q_{\text{EA}} = D_{aa}(\tau \rightarrow \infty)$.

The problem defined by Eqs. (2,3) is still too complicated to be solved exactly, even in the paramagnetic phase. However, it can be related to a solvable problem, which can be shown to have the same qualitative phase diagram and the same low-frequency and low-temperature universal properties. To arrive at this solvable model, we have to go through two additional steps. The first one is to “integrate out” conduction electrons in S_{eff} , so that an action involving only spin degrees of freedom is obtained. This cannot be done exactly because of the Kondo interaction, but can be done asymptotically at low energies by following the classic Anderson-Yuval-Hamann approach to the Kondo problem.¹⁰ This approach consists in separating the Kondo term into an Ising part $S^z s^z$ and a spin-flip part, and performing an expansion in the spin-flip term to all orders. The result of this procedure is a mapping of the Kondo part of S_{eff} onto an action involving an effective interaction for the Ising components of the spins. This effective interaction is retarded and decays as $1/\tau^2$ for large (imaginary time) separations τ . Thus low-energy properties of the model can be studied by replacing S_{eff} with

$$\begin{aligned}
S'_{\text{eff}} = & \int_0^\beta d\tau \int_0^\beta d\tau' \sum_{a,b} S_a^z(\tau) [K(\tau - \tau') \delta_{ab} \\
& - J^2 D_{ab}(\tau - \tau')] S_b^z(\tau'),
\end{aligned} \tag{4}$$

in which $K(\tau) \sim 1/\tau^2$ at large τ , i.e., $K(i\omega_n) \sim \kappa \omega_n \text{sgn}(\omega_n)$ (κ is a dimensionless parameter depending on the anisotropy of the Kondo coupling). This behavior must be cut off at high frequency $\omega > \Lambda$ (i.e., at short time separation). Because the decay $K(\tau) \sim 1/\tau^2$ only holds for times longer than $1/T_K$, where T_K is the “bare” Kondo temperature in the absence of the exchange J , the cutoff must be chosen as $\Lambda \simeq T_K$. This

slow decay of $K(\tau)$ stems from the metallic nature of the spin-glass problem under consideration. In the insulating case considered in Refs. 11, 12, the decay is faster with $K(i\omega_n) \sim \omega_n^2$.

III. SOLUTION AND PHYSICAL PROPERTIES

A. Solvable $M = \infty$ limit

In order to analyze the effective action (4), we can follow Ye, Sachdev, and Read¹² and generalize the model from Ising spins to M -components quantum rotors $\hat{n}_{i\mu}$, $\mu = 1, \dots, M$, with $\hat{n}_i^2 = 1$ at each site. The Ising case formally corresponds to $M = 1$, but the $M \rightarrow \infty$ limit will be first solved exactly. Enforcing the local constraint by Lagrange multipliers λ_j , the model is solved in this limit by a saddle-point method,¹² with $i\lambda_j \equiv \lambda$ uniform at the saddle point. The free energy of the model reads, in the paramagnetic (replica symmetric) phase,

$$\frac{F}{NM} = \lambda + \frac{1}{2\beta} \sum_n \ln[\lambda + K(i\omega_n) - J^2 D(i\omega_n)], \tag{5}$$

where the spin-correlator $D(i\omega_n)$ is given by

$$D(i\omega_n) = \frac{1}{2J^2} \{ \lambda + K(i\omega_n) - \sqrt{[\lambda + K(i\omega_n)]^2 - 4J^2} \}. \tag{6}$$

The Lagrange multiplier λ is determined by the constraint equation (equivalent to setting $\partial F/\partial \lambda = 0$):

$$-\frac{1}{2\beta} \sum_n D(i\omega_n) = 1. \tag{7}$$

B. Connection with $z = 2, d = 3$ quantum-critical phenomena

In order to analyze the phase diagram and critical behavior resulting from these equations, it is very useful to put them in a different form, which will reveal a connection with a different problem already analyzed in the literature. Indeed, instead of using a mapping onto the single-site action (4), we could have solved the $M = \infty$ rotor model directly for the fully connected lattice. In this approach, the spin-spin correlation function $D(i\omega_n)$ is given by the on-site component of the inverse of the random matrix: $[\lambda + K(i\omega_n)]\delta_{ij} - J_{ij}$. In the thermodynamic limit $N = \infty$, the eigenvalues of the matrix J_{ij} have a semicircular distribution given by

$$\rho_J(x) = \frac{1}{2\pi J^2} \sqrt{4J^2 - x^2} \theta(2J - |x|). \tag{8}$$

Hence the free-energy and spin propagator can be written in the equivalent form:

$$\frac{F}{MN} = \lambda + \sum_n \int_{-2J}^{+2J} dx \rho_J(x) \ln[\lambda + K(i\omega_n) - x], \tag{9}$$

$$D(i\omega_n) = \int_{-2J}^{+2J} dx \frac{\rho_J(x)}{\lambda + K(i\omega_n) - x}. \quad (10)$$

Independently of the low-frequency behavior of $K(i\omega_n)$ (metallic or insulating), it is clear that only the solutions with $\lambda \geq 2J$ are admissible¹² (so that no pole is encountered in the integration over x). The critical boundary with the spin-glass phase is signaled by $\lambda(T, J)$ reaching the value $2J$ [the condition $\lambda(T, J) = 2J$ holds throughout the spin-glass phase]. Thus the combination $\Delta \equiv \lambda - 2J$ plays the role of the important low-energy scale (which vanishes in the spin-glass phase). Universal low-frequency properties are found when this energy scale is small. These universal properties only depend on the low-frequency behavior of $K(i\omega_n)$ and on the fact that the spectral density $\rho_J(x)$ has a square-root behavior near its upper band edge $+2J$. Formally, this behavior is identical to that of fermions with a kinetic energy proportional to k^2 in $d = 3$ dimensions: we could as well set $K(i\omega_n) + \lambda - x \equiv K(i\omega_n) + \Delta + k^2$ and replace the integration over x in the above equations by an integration over d^3k (with some upper cutoff). In this analogy, the scaling of frequency with respect to k is obtained from $K(i\omega_n) \sim \omega_n^2 \sim k^2$ in the insulating case of Ref. 12, while $K(i\omega_n) \sim |\omega_n| \sim k^2$ in the metallic case. Therefore, we conclude that there is a formal equivalence with quantum-critical phenomena^{13–15} in the $d = 3, z = 1$ universality class for the insulating case, and in the $d = 3, z = 2$ universality class for the metallic case of interest here. The insulating case considered in Ref. 12 corresponds to a (quantum) Landau-Ginzburg model at its upper critical dimension $d+z = 4$ (with ϕ^4 a marginal perturbation), while the metallic case amounts to look at this model above its upper critical dimension (with ϕ^4 a dangerously irrelevant perturbation). For these reasons, many results that will be derived below for the metallic case are formally identical to those of Millis¹⁵ for the $d = 3, z = 2$ case.

In order to derive these results, it is most useful to convert the Matsubara sums in the above equations into real-frequency integrations. Using $K(\omega + i0^+) \sim i\omega \operatorname{sgn}(\omega)$ (with an upper cutoff Λ), we can write the free energy as

$$\frac{F}{NM} = \lambda + \int_0^\Lambda \frac{d\omega}{\pi} \coth \frac{\beta\omega}{2} \int_{-2J}^{+2J} dx \rho_J(x) \tan^{-1} \frac{\omega}{\lambda - x} \quad (11)$$

and the constraint equation reads

$$\int_0^\Lambda d\omega \chi''(\omega) \coth \frac{\beta\omega}{2} = 1, \quad (12)$$

with

$$\begin{aligned} \chi''(\omega) &\equiv -\frac{1}{\pi} \operatorname{Im} D(\omega + i0^+) \\ &= \operatorname{sgn}(\omega) \int_{-2J}^{+2J} dx \rho_J(x) \frac{\omega}{\pi[\omega^2 + (\lambda - x)^2]}. \end{aligned} \quad (13)$$

C. Phase diagram

The phase diagram resulting from Eqs. (12,13) is depicted schematically in Fig. 1. It is qualitatively similar to the insulating case,¹² but the equations for the critical boundary and the various crossover lines are affected by the different low-frequency behavior of $K(i\omega_n)$. Some calculations are detailed in the Appendix. For very large J , the spin-glass transition temperature is at $T_c = J$, the classical value.⁶ T_c decreases upon increasing quantum fluctuations (i.e., increasing J_K) and eventually vanishes for J smaller than a critical value: $J_c \simeq \Lambda \kappa^{1/3} \simeq T_K \kappa^{1/3}$. Near zero temperature, the phase boundary is such that $1 - J_c(T)/J_c \sim (T/\Lambda)^{3/2} \sim (T/T_K)^{3/2}$ (to be contrasted with $\sim T^2$ in the insulating case¹²).

Next, we discuss the various crossover regimes¹⁵ near the $T = 0$ quantum critical point at $J = J_c$ (cf. Fig. 1). Close to this point, and for low frequency and small Δ (but ω/Δ arbitrary), the imaginary part of the local dynamical susceptibility $\chi''(\omega) = -1/\pi \operatorname{Im} D(\omega + i0^+)$ takes the scaling form

$$\chi''(\omega) = \frac{C}{J_c^{3/2}} \operatorname{sgn}(\omega) \sqrt{|\omega|} f\left(\frac{\omega}{\Delta}\right). \quad (14)$$

The scaling function $f(x)$ is easily obtained from (6) as

$$f(x) = \left[x/(1 + \sqrt{1 + x^2}) \right]^{1/2} \quad (15)$$

and behaves as $f(x) \sim 1$ for $x \rightarrow \infty$ and $f(x) \sim \sqrt{x}$ for $x \rightarrow 0$. Hence spin excitations are gapless in all regimes, with $\chi''(\omega) \sim \omega/(J_c^{3/2} \sqrt{\Delta})$ for $\omega \ll \Delta$ and $\chi''(\omega) \sim \operatorname{sgn}(\omega) \sqrt{\omega}/J_c^{3/2}$ for $\omega \gg \Delta$. The former, linear behavior is characteristic of local spin correlations in a Fermi liquid with a low-energy scale Δ , while the latter (which holds down to $\omega = 0$ at the $T = 0$ critical point) deviates

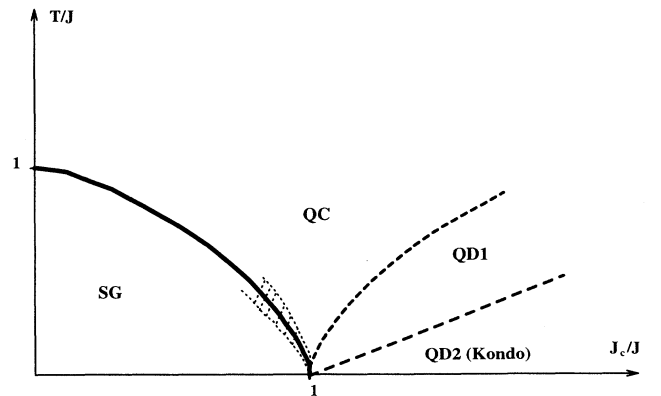


FIG. 1. Schematic phase diagram at mean-field level, as a function of T/J and J_c/J (with $J_c \simeq \Lambda \simeq T_K$). The plain line is the critical boundary with the spin-glass phase. All other lines are crossover lines, corresponding to the regimes described in the text. The hatched region is that of classical behavior near the critical boundary.

strongly from Fermi-liquid theory. C is a nonuniversal constant, and the low-energy scale $\Delta(T, J) \equiv \lambda - 2J$ has different behavior in different regions of the phase diagram (Fig. 1). $\Delta = 0$ inside the spin-glass phase, in which $\chi''(\omega) \sim \text{sgn}(\omega)\sqrt{\omega}$ with no characteristic scale.

Raising temperature at $J = J_c$, one enters the *quantum critical* (QC) regime, in which the physics is dominated by the $T = 0$ quantum critical point. The energy scale $\Delta \equiv \lambda - 2J$ is set entirely by temperature in this regime and is found to be $\Delta \sim T^{3/2}/\sqrt{J_c} \sim T^{3/2}/\sqrt{T_K}$. One would have naively expected $\Delta \sim T$ but we find a *violation of this scaling* in the QC regime of this model. Following the connection explained above, this is an effect of the ϕ^4 term in the quantum Landau-Ginzburg model being a dangerously irrelevant perturbation for $d + z = 5 > 4$.

Decreasing J (or increasing T_K) from the $T = 0$ critical point, at low enough temperature, one enters the *quantum disordered* (QD) regime in which $\Delta \sim J_c - J \sim T_K - J$ (to dominant order). The crossover between the QC and QD regimes occurs at $J = J^*(T)$ obtained by matching the two behaviors of Δ given above with the result $1 - J^*(T)/J_c \sim (T/J_c)^{3/2} \sim (T/T_K)^{3/2}$. As shown below, two distinct regions corresponding to $T \gg \Delta$ and $T \ll \Delta$ must actually be distinguished within the QD regime, in which the physical quantities have quite different low-temperature behavior. In the low-temperature region of the QD regime (denoted QD₂ on Fig. 1), the physics is that of a metal showing Fermi-liquid behavior below the coherence scale (or *effective* Kondo scale) Δ , which can be very small because of the competition between the Kondo effect and the freezing of the local moments. However, this interpretation has to be handled with some care, since this scale enters the various physical quantities in quite different manners, as detailed below.

Finally, near the phase boundary, there is a *classical* regime¹⁵ for $|J - J_c(T)| \ll T^2/J_c$ dominated by purely classical fluctuations and in which $\Delta \sim J_c[J - J_c(T)]^2/T^2$.

D. Specific heat, susceptibility, and NMR relaxation rate

We now investigate the low-temperature behavior of the specific heat in the various regimes described above. Some details of the calculation are provided in the Appendix, but the results could also be directly read off from those in Ref. 15, given the equivalence with the $d = 3, z = 2$ problem. In the QC regime, the specific-heat coefficient $\gamma \equiv C/T$ is found to behave as

$$\gamma = \gamma_0 - \frac{A}{J_c^{3/2}} \sqrt{T} + \dots \quad (16)$$

Interestingly, the non-Fermi-liquid nature of the quantum-critical point results in a nonanalytic correction to the low-temperature specific heat in this regime. Very close to the critical boundary with the spin-glass phase, there is an additional contribution:¹⁵ $BT/[J - J_c(T) +$

$T^{3/2}]^{1/2}$ [$\sim T^{1/4}$ for $J \simeq J_c(T)$], which becomes rapidly negligible, however, as one moves away from the critical boundary.

The nonanalytic \sqrt{T} behavior continues to hold within the QD regime as long as $T \gg \Delta$, i.e., $T \gg J_c - J$. This defines an additional subdivision of the QD regime, corresponding to region QD₁ in Fig. 1. In the low-temperature (QD₂) region of the QD regime, (16) is replaced by

$$\gamma = \gamma_0 - \frac{C}{J_c^{3/2}} \sqrt{\Delta} - \frac{D}{J_c^{3/2}} \frac{T^2}{\Delta^{3/2}} + \dots, \quad (17)$$

with $\Delta \sim J_c - J$ and where $\gamma_0 \propto 1/J_c$ remains finite as $J \rightarrow J_c$.

Next, we discuss the low-temperature behavior of the uniform spin susceptibility χ . This quantity is assumed to be measured by applying a uniform field such that the Zeeman energy μH is smaller than the bare Kondo scale T_K . Then the Kondo effect still takes place and the low-frequency behavior of the resulting propagator $K(i\omega_n)$ is essentially unaffected. We can thus simply introduce a uniform magnetic field $H \sum_i S_i^z$ in the effective Ising model. The susceptibility is given by the sum over all pairs of sites of the spin-spin correlation function taken at $\omega_n = 0^+$, namely

$$\chi = \sum_{ij} \overline{[\lambda + K(i0^+) - J_{kl}]_{ij}^{-1}}. \quad (18)$$

In this expression, the overbar denotes an averaging over disorder. The inverse of the random matrix present in this expression can be evaluated by expanding in powers of J_{kl} . Because these couplings have random signs and zero mean, only closed paths (with $i = j$) give a nonzero contribution on the fully connected (or Bethe) lattice. Hence the uniform susceptibility behaves in an identical manner to the *local* spin susceptibility: $\chi_{\text{loc}} = \int_0^\beta d\tau D(\tau)$. Note that this relies crucially on the fact that we are dealing with a random system, and would not apply to a uniform antiferromagnet for example. Hence the formal analogy between the present problem and the $z = 2, d = 3$ quantum antiferromagnet *does not apply* to the calculation of the susceptibility. χ_{loc} (and thus χ) is easily obtained by setting $\omega_n \rightarrow 0^+$ in Eq. (6) and taking the real part. This yields $2J^2\chi_{\text{loc}} = \text{const} - 2[J\Delta(T, J)]^{1/2} + \Delta(T, J)$.

In the QC regime, we must set $\Delta \sim T^{3/2}$, so that

$$\chi(T) = \chi_0 \left[1 - a \left(\frac{T}{J_c} \right)^{3/4} + \dots \right], \quad (19)$$

with $\chi_0 \sim 1/J_c$, and c a numerical constant. A non-analytic correction departing from standard Fermi-liquid theory is again found. In the high-temperature part of the QD regime (QD₁ region), we have (cf. Appendix) $\Delta(T) = \Delta + T^{3/2}$, so that

$$\chi(T) = \chi_0 - a_1 \frac{\sqrt{\Delta}}{J_c^{3/2}} - a_2 \frac{T^{3/2}}{J_c^2 \sqrt{\Delta}} + \dots \quad (20)$$

In the low-temperature (Kondo) region of the QD regime, we have (cf. Appendix) $\Delta(T) = \Delta + T^2/\sqrt{\Delta}$, so that

$$\chi(T) = \chi_0 - a_1 \frac{\sqrt{\Delta}}{J_c^{3/2}} - a_2 \frac{T^2}{J_c^2 \Delta} + \dots \quad (21)$$

In both (20) and (21), $\Delta \sim J_c - J$ and we emphasize that $\chi_0 \sim 1/J_c$ is nonsingular as the critical point is reached.

Finally, we consider the NMR relaxation rate, which is directly related to the $\omega = 0$ behavior of the local dynamical susceptibility through

$$\frac{1}{T_1 T} \equiv \frac{\chi''(\omega)}{\omega} \Big|_{\omega=0}. \quad (22)$$

Hence this quantity always feels the linear regime $\chi''(\omega) \sim \omega/\sqrt{\Delta}$ in the scaling form (14). In the QC regime, this yields a temperature dependence of the relaxation rate which differs from the usual Korringa behavior ($1/T_1 T \sim \text{const}$) found in a Fermi liquid:

$$\frac{1}{T_1 T} \sim \frac{1}{T^{3/4}}. \quad (23)$$

In contrast, in both the QD_1 and the QD_2 (“Kondo”) regime, the Korringa law is obeyed, but with an enhanced rate:

$$\frac{1}{T_1 T} \sim \frac{1}{\sqrt{\Delta}} \sim \frac{1}{\sqrt{J_c - J}}. \quad (24)$$

We emphasize that in the same regime, the $T = 0$ uniform spin susceptibility is *not* critically enhanced (the low-energy scale Δ only enters subleading corrections).

E. Ising ($M = 1$) case

Before leaving model (1), we would like to show that the Ising case $M = 1$ actually has the same universal low-frequency behavior than the rotor model in the $M \rightarrow \infty$ limit that we have analyzed in detail. In order to show this, one possibility is to adapt the reasoning of Refs. 11, 12 to the present case. Specifically, we can define the spin irreducible self-energy associated with (4) by $D(i\omega_n)^{-1} = K(i\omega_n) - J^2 D - \Pi(i\omega_n)$. For $M = \infty$, $\Pi(i\omega_n)$ reduces to a constant $\Pi = \lambda$. To order $1/M$, the first contribution to $\text{Im}\Pi$ is from decays into three spin waves. With $D(\tau) \sim 1/\tau^{3/2}$ at the critical point, this leads to $\text{Im}\Pi \sim \omega_n^{7/2}$. No nonanalyticity with a weaker power of frequency is induced to any order in $1/M$, and hence the low-frequency behavior found above at the critical point is unchanged. Another line of reasoning leading to the same conclusion is to use the formal equivalence with the $d = 3, z = 2$ universality class. Going from the $M = \infty$ to the $M = 1$ case just changes the specific coefficients of the various terms of the (quantum) Landau-Ginzburg model, but the equivalence holds for all M .

IV. MODEL WITH A SINGLE CONDUCTION ELECTRON FLUID AND TRANSPORT PROPERTIES

Finally, we shall release the assumption of independent Kondo baths at each site, and consider a model with a

single species of conduction electrons. We shall consider a lattice of connectivity z , and study the Hamiltonian

$$H_2 = - \sum_{ij\sigma} t_{ij} c_{i\sigma}^{\dagger} c_{j\sigma} + J_K \sum_i \vec{S}_i \cdot \vec{s}(i) - \sum_{(ij)} J_{ij} S_i^z \cdot S_j^z. \quad (25)$$

The random exchange couplings are distributed according to a Gaussian distribution as above, which is now normalized such that $\overline{J_{ij}^2} = J^2/z$. The limit of large lattice connectivity $z \rightarrow \infty$ will be considered below. In this limit, the various Green’s functions satisfy self-consistent dynamical mean-field equations.^{8,9} These equations reduce the model to the solution of a single-site effective action, which has again precisely the form in Eq. (2). However, there is now a self-consistency condition on *both* $D(i\omega_n)$ [given by Eq. (3) above] and $\mathcal{G}_0(i\omega_n)$, which is not known explicitly in contrast to the case above. This self-consistency condition depends on the specific lattice and hopping term t_{ij} . More precisely, if $D(\epsilon)$ stands for the noninteracting density of states of the lattice under consideration, the effective propagator \mathcal{G}_0 must be such that the following self-consistency equation holds:^{8,9}

$$G_c(i\omega_n) = \int_{-\infty}^{+\infty} d\epsilon \frac{D(\epsilon)}{i\omega_n + \mu - \Sigma_c(i\omega_n) - \epsilon}. \quad (26)$$

In this equation, G_c stands for the local conduction electron Green’s function $G_c = -(Tcc^{\dagger})_{S_{\text{eff}}}$, and Σ_c for the self-energy $\Sigma_c \equiv \mathcal{G}_0^{-1} - G_c^{-1}$. Both should be viewed as functionals of $\mathcal{G}_0(i\omega_n)$ [and $D(i\omega_n)$].

A first possibility is to consider a model with a specific form of *long-range* hopping (described in Ref. 9), such that the noninteracting conduction electron density of states is a Lorentzian $D(\epsilon) = 1/\pi(\epsilon^2 + \Gamma^2)$. In this case, the Hilbert transform in (26) yields $G_c = [i\omega_n + \mu - \Sigma_c + i\Gamma \text{sgn}(\omega_n)]^{-1}$, so that Σ_c disappears altogether from the self-consistency equation and \mathcal{G}_0 is actually known explicitly as before: $\mathcal{G}_0^{-1} = i\omega_n + i\Gamma \text{sgn}(\omega_n)$. Hence *exactly the same equations* as in the above model (1) with independent Kondo baths are found for this model with long-range hopping, and no nontrivial feedback of the conduction electron dynamics into the spin dynamics is possible.

The situation is different for a model with *short-range hopping* of the conduction electrons. For definiteness (but without loss of generality), we may consider the $z = \infty$ Bethe lattice, with nearest-neighbor hopping normalized according to $t_{ij} = t/\sqrt{z}$. (This corresponds to a semicircular density of states with a half-width $2t$.) In this case, (26) takes the simpler form

$$\mathcal{G}_0^{-1}(i\omega_n) = i\omega_n + \mu - t^2 G_c(i\omega_n). \quad (27)$$

G_c has to be determined from the solution of S_{eff} itself, so that the problem involves a self-consistency condition on *both* $D(i\omega_n)$ and $\mathcal{G}_0(i\omega_n)$. The main question is whether this “feedback” of the nontrivial spin dynamics into \mathcal{G}_0 can change the low-frequency behavior of $\chi''(\omega)$ at the $T = 0$ critical point. We shall give an argument that this is not the case, and that (14) still holds.

Let us imagine that the coupled problem (2,3,27) is solved iteratively, starting from a \mathcal{G}_0 which has the same long-time behavior than in the model without feedback, namely $\mathcal{G}_0(\tau) \sim 1/\tau$. Then, the arguments above yield $D(\tau) \sim 1/\tau^{3/2}$ at the critical point. Inserting this into the effective action (2), we have to compute the conduction electron Green's function G_c and feed it back into the self-consistency condition (27) to see how \mathcal{G}_0 is affected. In order to find the behavior of G_c , it is convenient to use a representation of the localized spins by pseudofermions f_σ , such that $\vec{S} = f_\sigma^+ \vec{\sigma}_{\sigma\sigma'} f_\sigma/2$. This amounts to "undoing" the Schrieffer-Wolff transformation and representing the original Kondo lattice as a periodic Anderson model with a very large U in the local moment limit $\epsilon_f \simeq -U/2$. We shall not attempt here to find the actual behavior of the f -electrons Green's functions $G_f(\tau)$, but it is easily seen that it cannot decay faster than $1/\tau^{3/4}$. Indeed, $D(\tau)$ always contains a term of the form $G_f(\tau)G_f(-\tau)$ (supplemented by vertex corrections), so that a decay slower than $1/\tau^{3/4}$ is inconsistent with $D(\tau) \sim 1/\tau^{3/2}$. Furthermore, the slowest possible decay of $G_f(\tau)$ is the Fermi-liquid form $G_f(\tau) \sim 1/\tau$. Hence we conclude that $G_f(\tau) \sim 1/\tau^\theta$, with the exponent θ such that $3/4 \leq \theta \leq 1$. Now, the t matrix associated with (2) is proportional to $G_f(i\omega_n)$, so that the conduction electron Green's function is given by $G_c(i\omega_n) = \mathcal{G}_0(i\omega_n) + V^2 \mathcal{G}_0(i\omega_n)^2 G_f(i\omega_n)$. Hence $G_c(\omega)$ behaves as $\omega^{\theta-1}$ at low frequency. Inserting this into the self-consistency equation (27) in order to see how \mathcal{G}_0 is affected at the next step of the iteration, we see that $\mathcal{G}_0(\tau)$ behaves as $1/\tau^{2-\theta}$ for large τ . Because of the constraint above, this exponent satisfies the bounds $1 \leq 2-\theta \leq 1+1/4$, so that \mathcal{G}_0 cannot decay faster than $1/\tau$ at the next iteration. Hence the associated spectral density $\text{Im}\mathcal{G}_0(\omega+i0^+)$ cannot diverge at $\omega=0$: it is either finite or vanishes. For large enough Kondo coupling, this yields a standard Kondo effect,¹⁶ and hence an effective interaction between Ising spins such that $K(\tau) \sim 1/\tau^2$ as before, so that the behavior of $\chi''(\omega)$ at the critical point remains unchanged at any step of the iterative solution of the coupled equations.

A perturbative argument can actually be given that the dominant behavior $G_c(\tau) \sim 1/\tau$ of the conduction electron Green's function is not affected at the $T=0$ critical point, i.e., that $\theta=1$. Indeed, if we treat the residual coupling between the conduction electrons and localized spins in second-order perturbation theory, we obtain a contribution to the self-energy: $\Sigma_c(\tau) \propto J_K^2 D(\tau) \mathcal{G}_0(\tau) \sim 1/\tau^{5/2}$, so that $\Sigma_c(\omega)$ behaves as $\omega^{3/2}$ at $T=0$. Hence this scattering is unable to modify the dominant term in the long-time behavior of $G_c(\tau) \sim 1/\tau$.

It has, however, important consequences for the transport properties near the $T=0$ critical point, as we shall now show. We first perform a more precise evaluation of the finite-temperature scattering rate to order J_K^2 , which takes the form

$$\text{Im}\Sigma_c(\omega+i0^+) \propto J_K^2 \rho_0(0) \int_{-\infty}^{+\infty} du \chi''(u) \left(\frac{1}{e^{\beta u} - 1} + \frac{1}{e^{\beta(u+\omega)} + 1} \right). \quad (28)$$

Inserting the scaling form (14), this leads to the following low-frequency and low-temperature dependence, in the quantum-critical regime:

$$\text{Im}\Sigma_c(\omega+i0^+) \propto \frac{J_K^2}{J_c^{3/2}} \rho_0(0) [\omega^{3/2} + T^{3/2}], \quad (29)$$

while in both regions of the QD regime:

$$\text{Im}\Sigma_c(\omega+i0^+) \propto \frac{J_K^2}{J_c^{3/2}} \rho_0(0) \left[\frac{\omega^2}{\sqrt{\Delta}} + \frac{T^2}{\sqrt{\Delta}} \right]. \quad (30)$$

Since we are dealing with a model on a lattice with infinite connectivity, the vertex corrections to the conductivity vanish,¹⁷ and the dc conductivity is simply given by

$$\sigma_{\text{dc}} \propto \int d\epsilon D(\epsilon) \times \int d\omega \frac{\text{Im}\Sigma_c(\omega)}{(\omega + \mu - \text{Re}\Sigma_c - \epsilon)^2 + (\text{Im}\Sigma_c)^2} \frac{\partial f}{\partial \omega}. \quad (31)$$

Hence the above calculation of the scattering rate leads to the following non-Fermi-liquid temperature dependence of the resistivity in the QC regime:

$$\delta\rho(T) \sim T^{3/2}, \quad (32)$$

while in both regions of the QD regime:

$$\delta\rho(T) \sim \frac{T^2}{\sqrt{\Delta}} \quad (33)$$

with $\Delta \sim J_c - J$. Hence a Fermi-liquid behavior $\delta\rho = AT^2$ is recovered in the QD regime, but with a critically enhanced rate $A \sim 1/\sqrt{\Delta}$. We emphasize that in the same regime, the specific heat coefficient γ is *not* critically enhanced. This distinguishes the QD Fermi-liquid regime from conventional heavy-fermion behavior in which *both* A and γ are large for small T_K , with¹⁸ $A \propto \gamma^2$.

V. CONCLUSION

In this paper, we have studied Kondo lattice models with a quenched random exchange between localized spins. The mean-field phase diagram has been investigated (Fig. 1) and found to display several different regimes near the quantum-critical point associated with the $T=0$ spin-glass transition. In the "quantum critical" regime, the specific heat coefficient and susceptibility display nonanalytic corrections to Fermi-liquid behavior given by (16,19), while the NMR relaxation rate (23) and resistivity (32) have a non-Fermi-liquid temperature dependence. In this regime, the important low-energy scale violates naive scaling and varies as a power of temperature ($\Delta \sim T^{3/2}$ at mean-field level). In the low-temperature part of the quantum-disordered region ("Kondo regime"), Fermi-liquid behavior is recovered, but the NMR and scattering rate are critically enhanced as the transition is reached, while γ and χ are not.

These results may have qualitative relevance for $Y_{1-x}U_x\text{Pd}_3$ and related systems^{1,3} since they indicate

that non-Fermi-liquid behavior is a rather generic feature associated with a $T = 0$ spin-glass transition in a metallic system. However, the reported experimental behavior ($\gamma \sim -\ln T$, $\chi = \chi_0 - \sqrt{T}$, $\delta\rho \sim T$) is not in good agreement with our mean-field results. This raises theoretical questions associated with the fluctuations beyond mean field, and also experimental questions concerning the actual investigation of the critical scaling regime.

Note added. As this work was being completed, we became aware of a work by S. Sachdev, N. Read, and R. Oppermann¹⁹ in which the phase diagram and crossovers described here are also analyzed, and a detailed theoretical investigation of the fluctuations beyond mean field is performed.

ACKNOWLEDGMENTS

A.S. would like to acknowledge a discussion with S. Sachdev on these topics, and the hospitality of Yale University on this occasion. We would also like to thank D. Huse and A. Millis for useful discussions.

APPENDIX

In this appendix, we provide some details on the analysis of the various crossovers and on the calculation of the specific heat. The starting point is the Eqs. (11,12,13) in which we set $\Delta \equiv \lambda - 2J$ and change variables in the integrations over x by setting $x = 2J - \epsilon$.

We shall deal first with the constraint, Eq. (12), which reads [replacing $\rho_J(x)$ by its square-root form near the upper band edge]

$$1 = \int_0^\Lambda \frac{d\omega}{\pi} \int_0^{4J} \frac{d\epsilon}{\pi J^{3/2}} \sqrt{\epsilon} \coth \frac{\beta\omega}{2} \frac{\omega}{\omega^2 + (\epsilon + \Delta)^2}. \quad (\text{A1})$$

The integral over ω needs to be cut off at $\Lambda \sim T_K$, while the integration over ϵ is ultraviolet convergent and its upper limit could as well be set to $+\infty$. We shall focus on the regions where $\Delta \ll T$ (which includes the QC regime and the upper part of the QD regime). Under this assumption, an expansion in Δ can be performed to yield

$$1 = \int_0^\Lambda \frac{d\omega}{\pi} \int_0^{4J} \frac{d\epsilon}{\pi J^{3/2}} \sqrt{\epsilon} \coth \frac{\beta\omega}{2} \left(\frac{\omega}{\omega^2 + \epsilon^2} - \Delta \frac{2\omega\epsilon}{(\omega^2 + \epsilon^2)^2} + O(\Delta^2) \right). \quad (\text{A2})$$

In the integrations over ϵ , we set $\epsilon = u\omega$ so that the ω dependence becomes apparent. Then, we use $\coth\beta\omega/2 = 1 + 2/(e^{\omega/T} - 1)$ and expand the integrals involving the last term at low temperature. The constraint equation then takes the form

$$1 = A_1 \left(\frac{\Lambda}{J} \right)^{3/2} + A_2 \left(\frac{T}{J} \right)^{3/2} - \frac{\Delta}{J} \left[B_1 \left(\frac{\Lambda}{J} \right)^{1/2} + B_2 \left(\frac{T}{J} \right)^{1/2} \right] + O(\Delta^2). \quad (\text{A3})$$

In this expression, the A_i 's and B_i 's are purely numerical, positive constants (independent of the cutoff and of J).

The location of the quantum critical point is readily obtained by setting $\Delta = T = 0$, yielding $J_c = A_1^{2/3} \Lambda \propto T_K$. When T is increased above this point, the behavior of Δ in the QC regime is found by canceling the dominant terms to next order, leading to $\Delta \sim A_2/B_1 T^{3/2}/\sqrt{\Lambda}$. The above expansion is valid as long as $\Delta \ll T$, so that we can also use it for $T^{3/2} \ll \Delta \ll T$, corresponding to the upper part of the QD region. In this case, we have to expand in $J = J_c - \delta J$ and the behavior $\Delta \sim \delta J + O(T^{3/2})$ is obtained. Also, the shape of the critical boundary at low temperature is found by expanding in $\delta J = J_c(T) - J_c$, with Δ set to 0. This yields $\delta J \propto T^{3/2}/\sqrt{J_c}$.

Next, we give some indications on the low-temperature expansion of the free energy in the QC regime. We rewrite Eq. (11) for the free-energy per site $f = F/NM$ under the form

$$f = \text{const} + \int_0^\Lambda \frac{d\omega}{\pi} \coth \frac{\beta\omega}{2} \times \int_0^{4J} \frac{d\epsilon}{\pi J^{3/2}} \sqrt{\epsilon} \tan^{-1} \frac{\omega}{\epsilon + \Delta}. \quad (\text{A4})$$

In the QC regime, we should use the following scaling variables: $\omega = T\tilde{\omega}$, $\epsilon = T\tilde{\epsilon}$, $\Delta = T^{3/2}\tilde{\Delta}$. Thus it is clear that Δ is the smallest energy scale, and we can simply expand the above expression in powers of Δ . The important point here is that *the linear term vanishes* because of the constraint equation above. Hence this expansion reads

$$f = \text{const} + \int_0^\Lambda \frac{d\omega}{\pi} \coth \frac{\beta\omega}{2} \int_0^{4J} \frac{d\epsilon}{\pi J^{3/2}} \sqrt{\epsilon} \left(\tan^{-1} \frac{\omega}{\epsilon} + \Delta^2 \frac{\omega\epsilon}{(\omega^2 + \epsilon^2)^2} + O(\Delta^3) \right). \quad (\text{A5})$$

The coefficient of the Δ^2 term is the same as found above in the analysis of the constraint. It leads to a dependence of the form $\Delta^2(\text{const} + \sqrt{T}) \sim T^3 + T^{5/2}$.

In order to find the temperature dependence of the first term, we make a low frequency expansion:

$$\int_0^{4J} \frac{d\epsilon}{\pi J^{3/2}} \sqrt{\epsilon} \tan^{-1} \frac{\omega}{\epsilon} \sim \frac{\omega}{J} + \left(\frac{\omega}{J} \right)^3 + O(\omega^3). \quad (\text{A6})$$

Hence this term yields a contribution of order $T^2 + T^{5/2}$ to the free energy. Overall, we find the low-temperature expansion

$$f \sim \text{const} + f_1 T^2 + f_2 T^{5/2} + \dots \quad (\text{A7})$$

in which the coefficients f_i 's are nonsingular and non-

vanishing as the critical point $J = J_c$ is reached. The behavior of $C = T\partial^2 f/\partial T^2 \sim \gamma_0 T - T^{3/2}$ follows.

Finally, we comment on the behavior of Δ in the low-temperature QD₂ regime. In this regime, the above expansions are no longer valid since they assumed $T \gg \Delta$. Concentrating, e.g., on the constraint equation, we see that the leading low-temperature correction is now controlled by the long-time behavior $D(\tau) \sim 1/\tau^2\sqrt{\Delta}$, which holds for $\tau\Delta \gg 1$. Using the Poisson summation formula, this yields

$$\begin{aligned} & \frac{1}{\beta} \sum_n D(i\omega_n)|_{J=J_c, T=0} - \frac{1}{\beta} \sum_n D(i\omega_n) \\ & = a\delta J + b\delta\lambda + c\frac{T^2}{\sqrt{\delta J}} + \dots, \quad (\text{A8}) \end{aligned}$$

with $\delta J = J - J_c$, $\delta\lambda = \lambda - 2J_c$. Canceling the leading corrections, one obtains $\Delta = J_c - J + \frac{T^2}{\sqrt{J_c - J}}$.

* Electronic address: anirvan@physics.att.com

† Electronic address: georges@physique.ens.fr

‡ Unité propre du CNRS (UP 701) associée à l'ENS et à l'Université Paris-Sud.

¹ M.B. Maple, M.C. de Andrade, J. Herrmann, Y. Dalichaouch, D.A. Gajewski, C.L. Seaman, R. Chau, R. Movshovich, M.C. Aronson, and R. Osborn, *J. Low Temp. Phys.* **99**, 223 (1995), and references therein.

² H. Von Lohneysen, T. Pietrus, G. Portisch, H. G. Schlager, A. Schroder, M. Sieck, and T. Trappmann, *Phys. Rev. Lett.* **72**, 3262 (1994).

³ C. L. Seaman, M. B. Maple, B. W. Lee, S. Ghamaty, M. S. Torikachvili, J. S. Kang, L. Z. Liu, J. W. Allen, and D. L. Cox, *Phys. Rev. Lett.* **67**, 2882 (1991).

⁴ D. L. Cox, *Phys. Rev. Lett.* **59**, 1240 (1987).

⁵ B. Andracka and A. M. Tsvelik, *Phys. Rev. Lett.* **67**, 2886 (1991).

⁶ D. Sherrington and S. Kirkpatrick, *Phys. Rev. Lett.* **35**, 1792 (1975).

⁷ A. J. Bray and M. A. Moore, *J. Phys. C* **13**, L655 (1980).

⁸ A. Georges and G. Kotliar, *Phys. Rev. B* **45**, 6479 (1992).

⁹ A. Georges, G. Kotliar, and Q. Si, *Int. J. Mod. Phys. B* **6**, 705 (1992).

¹⁰ P. W. Anderson, G. Yuval, and D. R. Hamann, *Phys. Rev. B* **1**, 4464 (1970).

¹¹ J. Miller and D. Huse, *Phys. Rev. Lett.* **70**, 3147 (1993).

¹² J. Ye, S. Sachdev, and N. Read, *Phys. Rev. Lett.* **70**, 4011 (1993); N. Read, S. Sachdev, and J. Ye, *Phys. Rev. B* **52**, 384 (1995).

¹³ J. A. Hertz, *Phys. Rev. B* **14**, 1165 (1976).

¹⁴ S. Sachdev and J. Ye, *Phys. Rev. Lett.* **69**, 2411 (1983).

¹⁵ A. J. Millis, *Phys. Rev. B* **48**, 7183 (1993); U. Zülicke and A. J. Millis, *Phys. Rev. B* **51**, 8996 (1995).

¹⁶ D. Withoff and E. Fradkin, *Phys. Rev. Lett.* **64**, 1835 (1990).

¹⁷ A. Khurana, *Phys. Rev. Lett.* **64**, 1990 (1990).

¹⁸ K. Kadowaki and S. B. Woods, *Solid State Commun.* **58**, 507 (1986); K. Miyake, T. Matsuura, and C. M. Varma, *ibid.* **71**, 1149 (1989).

¹⁹ S. Sachdev, N. Read, and R. Oppermann, preceding paper, *Phys. Rev. B* **52**, 10286 (1995).